

Global and regional
impacts of HONO on
aerosol composition

Y. F. Elshorbany et al.

This discussion paper is/has been under review for the journal Atmospheric Chemistry and Physics (ACP). Please refer to the corresponding final paper in ACP if available.

Global and regional impacts of HONO on the chemical composition of clouds and aerosols

Y. F. Elshorbany¹, P. J. Crutzen¹, B. Steil¹, A. Pozzer¹, H. Tost², and J. Lelieveld^{1,3}

¹Max Planck Institute for Chemistry, Division of Atmospheric Chemistry, Mainz, Germany

²Institut für Physik der Atmosphäre, Johannes Gutenberg Universität, Mainz, Germany

³The Cyprus Institute, Nicosia, Cyprus

Received: 22 July 2013 – Accepted: 26 August 2013 – Published: 9 September 2013

Correspondence to: Y. F. Elshorbany (yasin.elshorbany@mpic.de)

Published by Copernicus Publications on behalf of the European Geosciences Union.

Title Page

Abstract

Introduction

Conclusions

References

Tables

Figures

⏪

⏩

◀

▶

Back

Close

Full Screen / Esc

Printer-friendly Version

Interactive Discussion



Abstract

Nitrous acid (HONO) photolysis can significantly increase HO_x (OH+HO₂) radical formation, enhancing organic and inorganic oxidation products in polluted regions, especially during winter. It has been reported that chemistry-transport models underestimate sulphate concentrations, mostly during winter. Here we show that HONO can significantly enhance aerosol sulphate (S(VI)), mainly due to the increased formation of H₂SO₄. Even though in-cloud aqueous phase oxidation of dissolved SO₂ (S(IV)) is the main source of S(VI), it appears that HONO related enhancement of H₂O₂ does not significantly affect sulphate because of the predominantly S(IV) limited conditions, except over eastern Asia. Nitrate is also increased via enhanced gaseous HNO₃ formation and N₂O₅ hydrolysis on aerosol particles. Ammonium nitrate is enhanced in ammonia-rich regions but not under ammonia-limited conditions. Furthermore, particle number concentrations are also higher, accompanied by the transfer from hydrophobic to hydrophilic aerosol modes. This implies a significant impact on the particle lifetime and cloud nucleating properties. The HONO induced enhancements of all species studied are relatively strong in winter though negligible in summer. Simulating realistic HONO levels is found to improve the model-measurement agreement of sulphate aerosols, most apparent over the US. Our results underscore the importance of HONO for the atmospheric oxidizing capacity and the central role of cloud chemical processing in aerosol formation.

1 Introduction

Despite improvements in the control strategies of air quality in urban areas during the last decades, reducing air pollution is still a major challenge due to the very complex chemical system and the large number of species emitted into the atmosphere. Fine aerosol particles have direct and indirect impacts on climate (e.g., Charlson et al., 1991, 1992; Haywood and Boucher, 2000; IPCC, 2007) and human health (e.g., WHO, 2002;

Global and regional impacts of HONO on aerosol composition

Y. F. Elshorbany et al.

Title Page

Abstract

Introduction

Conclusions

References

Tables

Figures



Back

Close

Full Screen / Esc

Printer-friendly Version

Interactive Discussion



Global and regional impacts of HONO on aerosol composition

Y. F. Elshorbany et al.

Title Page

Abstract

Introduction

Conclusions

References

Tables

Figures

◀

▶

◀

▶

Back

Close

Full Screen / Esc

Printer-friendly Version

Interactive Discussion

Lelieveld et al., 2013). The aerosol radiative forcing is highly uncertain and depends on the aerosol burden and distribution (IPCC, 2007). Knowledge of aerosol chemical composition and the controlling processes are thus of paramount importance. The inorganic compounds SO_4^{2-} , NO_3^- and NH_4^+ are among the major constituents of the fine particles in polluted air, e.g., in megacities such as Beijing (Sun et al., 2013). Sulphate aerosols are primarily produced by the condensation of H_2SO_4 and the aqueous phase oxidation of dissolved gas phase SO_2 , S(IV), by O_3 and H_2O_2 (e.g., Lelieveld et al., 1997; Seinfeld and Pandis, 2006). Recently, the transition-metal-ion catalysed oxidation of S(IV) by O_2 has also been highlighted as an important source especially in rural areas (Harris et al., 2013 and references therein). Cloud processing has long been known as the most important source of aerosol sulphate on regional (e.g., Seidl and Dlugi, 1991; McHenry and Dennis, 1994; Lelieveld et al., 1997; Venkataraman et al., 2001; Menegoz et al., 2009) and global scale (e.g., Hegg, 1985; Feichter et al., 1996; Liao et al., 2003), accounting for up to two thirds of ambient sulphate concentrations, with H_2O_2 being the most effective oxidant followed by O_3 (e.g., Feichter et al., 1996). The aqueous phase oxidation of S(IV) can be either oxidant (i.e., O_3 or H_2O_2) or SO_2 limited and occurs primarily in clouds because of their relatively high liquid water content, LWC, compared to aerosol (e.g., Schwartz et al., 1987; Van den Berg et al., 2000; Seinfeld and Pandis, 2006). Under oxidant limited conditions, enhancement of the oxidant concentrations may significantly accelerate sulphate formation, in contrast to S(IV) limited conditions (e.g., Seinfeld and Pandis, 2006). Secondary aerosol formation by gas/liquid partitioning is also well recognised as an important source of aerosols (e.g., Kulmala et al., 2004). Sulphuric acid is the major contributor to atmospheric nucleation (e.g., Seidl and Dlugi, 1991; Kulmala et al., 2006; Kirkby et al., 2011; Neitola et al., 2013). Unlike sulphates, nitrates are nearly exclusively produced by the uptake of nitric acid (HNO_3) into cloud droplets and aerosols and its reaction with available ammonium and other cations. In ammonia-rich regions, enhancement of aerosol sulphate concentrations may also enhance nitrate aerosol formation via the heterogeneous N_2O_5 hydrolysis on sulphate aerosol particles forming HNO_3 (e.g., Lamsal et al.,

2010; L. Zhang et al., 2012). In ammonia-limited regions, enhancements of sulphate can substitute nitrate and chloride ions, driving them out of the condensed phase (e.g., Seinfeld and Pandis, 2006).

5 During the last decades, HONO has been shown to play a major role in HO_x (OH+HO₂) and O₃ production as well as in the formation of other secondary oxidation products (e.g., Perner and Platt, 1979; Harris et al., 1982; Elshorbany et al., 2009a, b, 2010a, b, 2012a, b). Several previous local-scale studies have reported an important impact of HONO photolysis on aerosol chemical composition. Goncalves et al. (2012) found that simulated PM_{2.5} is increased up to 14 % by accounting for HONO sources
10 in Madrid, Spain. Li et al. (2010) found that HONO sources play an important role in the formation of secondary aerosols in Mexico City, substantially enhancing their concentrations by a factor of 2 on average in the morning. They also found that the simulated particle-phase nitrate and ammonium are substantially enhanced in the morning, though the effect on sulphate aerosol was much smaller, being in good agreement with the measurements. Also, R. Zhang et al. (2012) found that HONO can enhance the
15 daily mean PM_{2.5} in the Pearl River Delta, China by up to 17 µg m⁻³ (12 %).

Underestimation of sulphate aerosols has been reported by several studies, especially in polluted regions, which was attributed to missing oxidation pathways, being largest in winter and relatively small in summer (e.g., Dennis et al., 1993; Roelofs et al., 1998, 2001). HONO formation mechanisms are still poorly understood and therefore it is difficult for global models to simulate realistic HONO concentrations. Recently, Elshorbany et al. (2012b) have shown that HONO levels can be realistically parameterized, being about an order of magnitude higher compared to the reference simulations that consider the reaction of OH+NO as the sole HONO source. They also showed that
20 HONO photolysis significantly enhances the gas phase mixing ratios of H₂O₂, HNO₃, O₃ and H₂SO₄, which play an important role in the formation of aerosols. Therefore, simulating realistic HONO levels may improve the agreement between models and measurements. In this study, we investigate the impact of HONO on the aerosol phys-

Global and regional impacts of HONO on aerosol composition

Y. F. Elshorbany et al.

Title Page

Abstract

Introduction

Conclusions

References

Tables

Figures

◀

▶

◀

▶

Back

Close

Full Screen / Esc

Printer-friendly Version

Interactive Discussion



ical and chemical properties and compare the simulation results with measurement data from monitoring networks.

2 Model description

The applied modelling system based on the ECHAM5 general circulation model (Roeckner et al., 2006) and the Modular Earth Submodel System (MESSy2, Jöckel et al., 2005, 2010) to simulates the meteorology and atmospheric chemistry. The ECHAM5/MESSy Atmospheric Chemistry (EMAC) system is a coupled lower-middle atmospheric chemistry general circulation model (AC-GCM), which has been extensively evaluated against observations (e.g., Jöckel et al., 2006; Lelieveld et al., 2007; Tost et al., 2007; Pozzer et al., 2007, 2010, 2012; Brühl et al., 2012; de Meij et al., 2012). The model structure and setup have been described by Jöckel et al. (2006) and (2010) and only a brief description is given here, focusing on aerosol related sub-models.

The atmospheric aerosol is parameterized in this study using the submodel GMXe (Pringle et al., 2010; Tost and Pringle, 2012). Gas/aerosol partitioning is calculated in GMXe in two stages; *kinetically* (the same as that in M7 (Vignati et al., 2004) but extended to NH_3 , HCl and HNO_3), in which the amount of gas phase species is kinetically allowed to condense (assuming diffusion limited condensation) on aerosol particles and *thermodynamically* (using ISORROPIA II, Fountoukis and Nenes, 2007), in which the condensed material is redistributed between the gas and aerosol phase. The size distribution (in radius) is described by four hydrophilic (nucleation (ns, < 5 nm), Aitken (ks, 5–50 nm), accumulation (as, 50–500 nm), coarse (cs, > 500 nm)) and three hydrophobic (Aitken (ki, 5–50 nm), accumulation (ai, 50–500 nm), coarse (ci, > 500 nm)) interacting lognormal aerosol modes, with prognostic aerosol mass and number and a diagnosed mean radius. The aerosol compounds treated explicitly are H_2O , Na^+ , Cl^- , NH_4^+ , SO_4^{2-} , NO_3^- and the bulk compounds of organic carbon (OC), black carbon (BC), dust and a bulk sea salt (the fraction that is not described by NaCl and sea salt

Global and regional impacts of HONO on aerosol composition

Y. F. Elshorbany et al.

Title Page

Abstract

Introduction

Conclusions

References

Tables

Figures

◀

▶

◀

▶

Back

Close

Full Screen / Esc

Printer-friendly Version

Interactive Discussion



Global and regional impacts of HONO on aerosol composition

Y. F. Elshorbany et al.

Title Page

Abstract

Introduction

Conclusions

References

Tables

Figures

◀

▶

◀

▶

Back

Close

Full Screen / Esc

Printer-friendly Version

Interactive Discussion



5 sulphate). Dry deposition, sedimentation and wet deposition of gas and aerosol phase species are calculated using DRYDEP (dry deposition of trace gases and aerosol particles, Ganzeveld et al., 1998; Kerkweg et al., 2006), SEDI (sedimentation of aerosol particles, Kerkweg et al., 2006), and SCAV (scavenging and liquid phase chemistry in clouds and precipitation, Tost et al., 2006) submodels, respectively. SCAV calculates the uptake of trace gases and aerosol particles (radius dependent) into cloud and precipitation droplets. The wet deposition flux out of the lowest model layer represents the chemical composition of rainwater. The gas and aqueous phase chemistry, including the transfer of gaseous compounds, dissociation of acidic and alkaline species in the droplets and aqueous phase redox reactions are calculated by a coupled system of ordinary differential equations using the kinetic pre-processor (KPP) software (Sandu and Sander, 2006). The gas and the liquid phase chemical processes are fully coupled and do not require prescribed mixing ratios or pH values. Since usually only a small fraction of a grid box is affected by clouds and precipitation, only the cloud covered part or the part in which the precipitation occurs contributes to the scavenging, while the rest of the grid box remains unaffected. A scavenged aerosol particle can be either removed from the atmosphere by wet deposition or released through droplet evaporation (aerosols are then transferred into the largest available mode). Ions that are converted to molecules via chemical reactions in the aqueous phase can be released to the gas phase. At the end of each time step, it is assumed that the cloud completely evaporates and that all volatile species will be released to the gas phase, while the ions are transferred to the aerosol phase, thus affecting the aerosol properties: e.g., the SO₂ oxidation to SO₄²⁻ can significantly increase the aerosol sulphate amount. Atmospheric gas phase chemical reactions are incorporated in the model through the module MECCA (Sander et al., 2005, 2011). To study the effects of changes in the chemistry while avoiding possible feedbacks of radiatively active gases and aerosols through the meteorology, the radiation scheme has been decoupled, and the model is used in the atmospheric chemistry-transport mode. The radiation code in EMAC uses

an ozone climatology (Fortuin and Kelder, 1998), fixed vertical profiles for CH₄, N₂O and CFCs and constant mixing ratios of CO₂.

The reference run (base_S1) has been performed for the years 2000–2001 in T42L31 resolution (i.e., with a triangular truncation at wave number 42 for the spectral core of ECHAM5, and with 31 levels on a hybrid-pressure grid in the vertical, reaching up to 10 hPa). The T42 resolution corresponds to a quadratic Gaussian grid of approximately 2.8° × 2.8° in latitude and longitude. To simulate realistic synoptic conditions, we applied a weak “nudging” towards actual meteorology by the assimilation of analysis data from the European Centre for Medium-range Weather Forecasting (ECMWF) through the Newtonian relaxation of four prognostic model variables: temperature, divergence, vorticity and the logarithm of surface pressure (van Aalst et al., 2004). The first 12 months of the simulation are regarded as a spin up period and these results are not considered in our analysis. In the sensitivity run S1, HONO levels were parameterized such that the HONO/NO_x ratio is fixed at 0.02, simulating realistic HONO levels (Elshorbany et al., 2012b). In order to investigate the most important process affected by the HONO enhancement in the model, four additional sensitivity runs were performed base_S2, S2, base_S3 and S3. In the base_S2 and S2 sensitivity runs, only gas/liquid partitioning based on Henry’ law coefficients was allowed without aqueous phase chemistry (similar to the “EASY” sensitivity runs in Tost et al., 2007), thus determining the impact of aqueous phase chemistry on aerosol formation in the absence (base_S2) and the presence (S2) of realistic HONO levels by comparing it to the base_S1 and S1 runs, respectively. In the base_S3 and S3 sensitivity runs, the gas phase oxidation of SO₂ with OH results in a dummy species (i.e., OH+SO₂ →DUMMY), thus masking the production of gas phase H₂SO₄. From these sensitivity runs, the impact of gas phase H₂SO₄ on the aerosol formation in the absence (base_S3) and the presence (S3) of realistic HONO levels can be determined by comparing them to the base_S1 and S1 runs, respectively.

The current study builds on the model-observation results of Elshorbany et al. (2012b) for the HONO parameterization and on the aerosol validation results of

Global and regional impacts of HONO on aerosol composition

Y. F. Elshorbany et al.

Title Page

Abstract

Introduction

Conclusions

References

Tables

Figures

◀

▶

◀

▶

Back

Close

Full Screen / Esc

Printer-friendly Version

Interactive Discussion



Global and regional impacts of HONO on aerosol composition

Y. F. Elshorbany et al.

Title Page

Abstract

Introduction

Conclusions

References

Tables

Figures

◀

▶

◀

▶

Back

Close

Full Screen / Esc

Printer-friendly Version

Interactive Discussion



OH and the gas phase oxidation products, HNO_3 ($\text{OH}+\text{NO}_2$), H_2SO_4 ($\text{OH}+\text{SO}_2$) and H_2O_2 (HO_2+HO_2) during winter are shown. The enhancement in HONO leads to increased oxidation rates by OH leading to enhancements in O_3 , N_2O_5 (not shown) and H_2O_2 and also to enhanced HNO_3 and H_2SO_4 levels, especially during winter (Fig. 2) while in summer much smaller enhancements are simulated. The enhancements of HNO_3 and H_2SO_4 increase nitrate and sulphate aerosols, respectively. In addition, the enhancement of aerosol sulphate also contributes to the formation of nitrates via the heterogeneous hydrolysis of N_2O_5 forming HNO_3 . The uptake of O_3 and H_2O_2 in clouds may enhance the aqueous oxidation of dissolved SO_2 in clouds, thus increasing the oxidation rates of HSO_3^- and SO_3^{2-} (S(IV)) to S(VI), which can be transferred to the aerosol phase upon the evaporation of the cloud droplets. However, the impact of HONO on the aqueous phase production of S(VI) depends on the relative abundance of S(IV) and the oxidants and does not affect sulphate concentrations under S(IV) limited conditions (Sect. 1). In the following sections, we investigate the impact of these enhanced gas phase species on the chemical composition of aerosols.

4.1 Impacts on aerosol chemical composition

The major constituents of fine aerosol particles are typically organic compounds (lumped as OC), water soluble ions, e.g., SO_4^{2-} , NO_3^- , and NH_4^+ , and mineral dust (Jimenez et al., 2009; Sun et al., 2013 and references therein). As mentioned above, daytime HONO photolysis accelerates oxidation processes, especially under high NO_x conditions, which leads to increased concentrations of aerosol precursors, e.g. HNO_3 , N_2O_5 , H_2SO_4 and other inorganic (e.g., O_3 , H_2O_2) and organic (OVOC, PAN) oxidation products, which can affect the cloud and aerosol composition.

4.1.1 Sulphates

As shown in Fig. 3, sulphate concentrations are higher in summer than in winter, related to the faster photochemical oxidation during summer. On the other hand, the

Global and regional impacts of HONO on aerosol composition

Y. F. Elshorbany et al.

Title Page

Abstract

Introduction

Conclusions

References

Tables

Figures

◀

▶

◀

▶

Back

Close

Full Screen / Esc

Printer-friendly Version

Interactive Discussion



5 impact of HONO is strongest during winter related to the relatively minor importance of other photolytic OH sources and the higher NO levels (i.e., conditions under which OH recycling is most efficient, see Sect. 4, Elshorbany et al., 2010b, 2012b). Aerosol sulphates are enhanced only in regions that are rich in both NO_x and ammonia; i.e.,
10 though India is an ammonia-rich region, sulphates are not significantly enhanced due to the relatively low-NO_x conditions in this region (see Fig. 3). Considering the growing NO_x sources in southern Asia this may change in future. The mean annual aerosol concentrations of sulphates (S(VI)) are significantly enhanced as a result of the more realistic HONO levels, reaching a mean annual relative enhancement of about 20 %
15 over the highly polluted NO_x-rich regions, especially over the eastern US and China. Furthermore, S(VI) is significantly enhanced during winter, reaching up to +50 % during January (Fig. 3).

As shown in Table 1, gas phase H₂SO₄ accounts for about 17–18 % of the simulated total sulphate aerosol concentration while aqueous phase chemistry accounts for about
20 25 and 54 % in January over the eastern US and China, respectively, in the base_S1 run. The remainder of the sulphate concentration is due to emissions (i.e., direct anthropogenic emissions and sea salt sulphate, see Pringle et al., 2010; Tost and Pringle, 2012). As a result of simulating realistic HONO levels (in the S1 run), the contribution of gas phase H₂SO₄ increases to about 30 and 26 % while that of the aqueous chemistry
25 decreases to 14 and 45 % over the eastern US and China, respectively. If only chemically formed sulphates are considered, gas phase H₂SO₄ would account for about 41 and 25 % of the simulated sulphate aerosol concentrations, which increases to about 68 and 37 % in January over the eastern US and China, respectively, as a result of simulating realistic HONO levels (see Table 1). Thus, the relative contribution of gas phase H₂SO₄ increases by about 69 and 50 % while that of the aqueous phase chemistry decreases by about 47 and 16 % over the eastern US and China, respectively. A striking result is that gas phase H₂SO₄ becomes more important than aqueous phase chemistry in sulphate production over the eastern US (see Table 1).

Global and regional impacts of HONO on aerosol composition

Y. F. Elshorbany et al.

Title Page

Abstract

Introduction

Conclusions

References

Tables

Figures

◀

▶

◀

▶

Back

Close

Full Screen / Esc

Printer-friendly Version

Interactive Discussion



In the absence of aqueous phase chemistry (Tables 1, S2), the enhancement of gas phase H_2SO_4 leads to about 31 and 34 % enhancement over the eastern US and China, respectively. In the absence of gas phase H_2SO_4 (Tables 1, S3), no significant sulphate enhancement is calculated. Thus, though both H_2O_2 and O_3 are also enhanced as a result of simulating realistic HONO levels (Fig. 2), they do not seem to significantly affect sulphate concentrations over the eastern US and China (see Table 1, S3). This is related to the prevailing S(IV) limited conditions in most of these regions, thus any increase in the H_2O_2 concentration does not affect sulphate aerosol concentration (cf. Seinfeld and Pandis, 2006; Shen, 2011). For instance, over eastern China, in the absence of H_2SO_4 from the gas phase oxidation of SO_2 , enhancement in the sulphate aerosol concentration (up to +50 %) seems to occur only when the ratio of $\text{H}_2\text{O}_2/\text{HSO}_3^-$ in the aqueous phase is below 0.1, while for ratios in excess of 1 (also over eastern US), no enhancements are calculated (Fig. 4).

In Table 2, the mean simulated concentrations of sulphate, nitrate and ammonium as well as their relative enhancements due to HONO are shown for the different soluble aerosol modes during summer and winter over the eastern US and China. The corresponding figures for the accumulation and coarse modes during winter are shown in Figs. 5 and 6, respectively. The relative enhancements in the aerosol mass concentrations are dominated by the nucleation and Aitken modes while the absolute enhancements are dominated by the accumulation mode and to a lesser extent the coarse mode. Since almost no enhancement in aerosol sulphate is calculated in the absence of the gas phase oxidation of SO_2 (Table 1, scenario S3), the enhancement in the larger modes is mainly related to the condensation of the enhanced gas phase H_2SO_4 as well as the coagulation of smaller particles in the nucleation and Aitken modes. Sulphate aerosol concentrations have been reported to be underestimated by models, especially during winter with much better correlation between measured and simulated sulphates during summer (Jeuken, 2000; Pringle et al., 2010; Pozzer et al., 2012; de Meij et al., 2012). This underestimation has been related to a possible lack of photochemical oxidation pathways of SO_2 , which, based on our results, could be due to the

underestimated OH during winter owing to the lack of HONO in their simulations (see Sect. 4.2).

4.1.2 Nitrates

In coastal regions nitrate aerosols are predominantly found as sodium nitrate and more inland (continental) as ammonium nitrate (if there is an excess of ammonia). Nitrates are generally overestimated by models compared to reported measurements, partly owing to experimental artefacts related to nitrate sampling on quartz filters, especially in spring and summer. Nevertheless, better correlations with measurements were observed in summer compared to winter, which were partly explained by the absence of oxidation pathways (de Meij et al., 2012; Pozzer et al., 2012). In contrast to sulphates, which are produced mainly by the oxidation of S(IV) with H_2O_2 and O_3 in clouds, nitrates are produced mainly from the transfer of gas phase nitric acid and N_2O_5 to the clouds/particles. The impact of enhanced gas phase HNO_3 levels on aerosol nitrate depends on the availability of ammonia/ammonium, which is preferentially bound by H_2SO_4 /sulphate (e.g., Seinfeld and Panids, 2006). In the absence of gas phase H_2SO_4 , nitrate concentrations are reduced by about 13 and 5% over eastern US and China, respectively, in the base run, which is related to the reduced surface area of sulphate aerosols allowing less condensation and hydrolysis (Tables 1, S3 compared to S1).

As shown in Figs. 5, 6 and 7, nitrate aerosols are enhanced only in polluted continental regions (ammonia-rich regions), while only marginally affected or even decreased in all other areas (ammonia-limited environments). Similar to aerosol sulphate, the enhancement in nitrate aerosol mass is dominated by the soluble accumulation and coarse modes (Table 2). Since most of the aerosol nitrate in the coastal and marine regions (ammonia-limited) is in the coarse mode, nitrate concentrations in this mode are suppressed owing to the enhancement in the sulphate concentrations while in the accumulation mode (mostly in continental polluted ammonia-rich environments) they are enhanced. Since HNO_3 is most strongly enhanced during winter, nitrate is also

Global and regional impacts of HONO on aerosol composition

Y. F. Elshorbany et al.

Title Page

Abstract

Introduction

Conclusions

References

Tables

Figures

◀

▶

◀

▶

Back

Close

Full Screen / Esc

Printer-friendly Version

Interactive Discussion



maximum relative enhancements are simulated in both regions during winter while during summer the enhancements are again negligible. The increase of aerosol number concentrations over eastern China reaches about 10^4 cm^{-3} during January, about one order of magnitude higher than that over the eastern US while during summer enhancements in both regions do not exceed 500 cm^{-3} (Fig. 11).

The mean simulated aerosol number concentration for the different aerosol modes over the eastern US and China are shown in Table 3. Aerosol number concentrations are dominated by the Aitken and accumulation modes, reflecting typical distributions of the near-surface aerosol number concentrations (see e.g., Pringle et al., 2010 and references therein). The mean relative enhancement in the total aerosol number concentrations over the eastern US and China is about 10–11 % (see Table 3). Another important effect is the transformation from hydrophobic to hydrophilic aerosols related mainly to the enhanced condensation of the gas phase constituents (e.g., H_2SO_4 , HNO_3) as well as the coagulation of the soluble new aerosol particles with the hydrophobic aerosol particles followed by transfer into the hydrophilic mode. For example, over eastern China the particle number in the hydrophobic Aitken (ki) mode is reduced by about 6 % (about 245 cm^{-3}) while that of the hydrophilic ks and as modes are enhanced by 31 and 14 %, respectively (total about 334 cm^{-3}).

Similarly, over the eastern US the hydrophobic Aitken mode particle number is reduced by 13 % (about 161 cm^{-3}) while the hydrophilic ks and as modes are enhanced by 44 and 27 %, respectively (total about 306 cm^{-3}), see Table 3. In the absence of gas phase H_2SO_4 , almost no enhancements in the total aerosol number concentrations are calculated as a result of realistic HONO levels. The total enhancement in the aerosol number concentrations can thus be attributed to the strong enhancement in the nucleation mode, especially over eastern China, related mainly to the enhancement in the gas phase sulphuric acid concentration (i.e., nucleation of new particles is calculated in the model as a function of the temperature, relative humidity and the concentration of gas phase H_2SO_4 , see Pringle et al., 2010).

Global and regional impacts of HONO on aerosol composition

Y. F. Elshorbany et al.

Title Page

Abstract

Introduction

Conclusions

References

Tables

Figures

◀

▶

◀

▶

Back

Close

Full Screen / Esc

Printer-friendly Version

Interactive Discussion



Global and regional impacts of HONO on aerosol composition

Y. F. Elshorbany et al.

Title Page

Abstract

Introduction

Conclusions

References

Tables

Figures



Back

Close

Full Screen / Esc

Printer-friendly Version

Interactive Discussion



It should however be mentioned that the transfer from the hydrophobic to hydrophilic modes, as a result of the enhanced gas phase H_2SO_4 , is not accompanied by an enhanced particle growth rate (i.e., the relative contributions of the different aerosol modes do not significantly change). These results are consistent with previous studies showing that nucleation and growth are almost decoupled, which is mainly due to the fact that the condensation of sulphuric acid does not explain the observed particle growth rate under most atmospheric conditions (Kulmala, 2003; Kulmala et al., 2000 and references therein). The enhancement of the aerosol number and solubility implies potential impacts on the cloud nucleation properties and particle lifetime. The enhancement of fine mode aerosol (nucleation, Aitken and accumulation mode) particles, as a result of simulating realistic HONO levels, may directly affect climate by increasing the light scattering and indirectly via altering cloud properties.

4.2 Comparison with large scale measurements

A summary of the comparisons between the mean simulated aerosol sulphates, nitrates and ammonium by the base_S1 and S1 model runs and the measurements by CASTNET, EMEP and EANET networks during winter (January to March) 2001 are listed in Table 4. As shown in Table 4, simulating realistic HONO levels (S1 simulations) generally increases the mean modelled/measured (MAM/OAM) ratio, most significantly over the US (about 20%), thus improving the agreement between modelled and measured sulphate concentrations in this region (i.e., modelled to observed ratio changes from 0.81 to 0.96). This is due to the enhanced gas phase oxidation of SO_2 , being most important over the eastern US, i.e., compared to eastern China (see Sect. 4.1.1 and Table 1). Simulated nitrate by both the base_S1 and S1 runs are generally overestimated with model/measured ratio ranges from 1.28 to 1.55. These overestimations of nitrate are however related to known issues, including measurement biases, overestimation of sea spray aerosols by GMXe, which may result in overestimation of aerosol nitrate by the uptake of HNO_3 (Pringle et al., 2010; de Meij et al., 2012). Over eastern Asia (EANET), the modelled/observed ratio for nitrate decreases from 1.55 for the base_S1

Global and regional impacts of HONO on aerosol composition

Y. F. Elshorbany et al.

Title Page

Abstract

Introduction

Conclusions

References

Tables

Figures

◀

▶

◀

▶

Back

Close

Full Screen / Esc

Printer-friendly Version

Interactive Discussion



to 1.41 for the S1 run (i.e., as a result of simulating realistic HONO levels). Ammonium aerosols are well simulated by the reference run over the US and eastern Asia (MAM/OAM are 0.98 and 1.01, respectively) while slightly overestimated over Europe, in agreement with Pringle et al. (2010). The ratio of simulated/measured ammonium aerosol generally follows that of sulphate and increases in the S1 run compared to the reference base_S1, especially over the US. Pozzer et al. (2012) investigated the EMAC simulation results for the years 2005–2008 and showed also that the model tends to underestimate sulphate aerosol compared to CASTNET and also compared to EMEP and EANET measurements. Furthermore, Pringle et al. (2010) compared simulated concentrations of sulphates, nitrates and ammonium fine mode aerosol ($< 1 \mu\text{m}$ diameter) concentrations with aerosol mass spectrometer data and found that the model tends to underestimate the three measured species with sulphates being most poorly captured. Since the HONO enhancements are most significant for the accumulation mode (see Table 2), it can be expected that with realistic HONO simulations, these simulated concentrations are in better agreement with the mass spectrometer measurements. They showed also that the EMAC model tends to overestimate nitrate in coastal regions, which (see Sect. 4.1.2) is more realistically simulated by improving the HONO simulation. Therefore, by accounting for realistic HONO levels the simulated aerosol concentrations are improved compared to measurements.

5 Conclusions

In this study the impact of our realistic HONO parameterization on the simulated aerosol composition has been investigated. By applying this parameterization, simulated HONO mixing ratios typically increase by an order of magnitude, in agreement with our previous study, which showed that this parameterization leads to much better agreement with measurements compared to the model run that only considers the reaction of $\text{NO} + \text{OH}$ as a source of HONO. Owing to the enhanced gas phase HONO photolysis, HO_x ($\text{OH} + \text{HO}_2$) levels are enhanced, thus promoting the formation of or-

ganic (e.g. PAN, OVOC) and inorganic (H_2O_2 , O_3 , HNO_3 and H_2SO_4) oxidation products in polluted regions, especially in winter when other photolytic HO_x sources are of relatively minor importance.

Simulating realistic HONO levels is found to significantly enhance the near surface aerosol sulphate concentrations, mainly due to enhanced gas phase oxidation of SO_2 with OH. Nitrate and ammonium are also significantly enhanced in ammonia-rich regions, while in ammonia-limited regions the effect is small. Furthermore, aerosol number concentrations are also significantly higher, accompanied by transfer from the hydrophobic to hydrophilic modes though without affecting the particle growth rate, which is mainly related to the condensation of H_2SO_4 on the hydrophobic particles. The enhancement of the aerosol number and solubility implies potential impacts on the cloud nucleating properties and the particle lifetime.

The relative enhancements of all species reach a maximum during the winter season while generally being negligible during summer. The simulation results are compared to data from the monitoring networks CASTNET, EMEP and EANET. The model results are in reasonable agreement with measurements and in line with previous evaluations. Simulating realistic HONO levels was found to enhance the species SO_4^{2-} , NO_3^- and NH_4^+ , with sulphates being most strongly enhanced, especially over the US, improving the agreement with measurements in this region. The results of the study underscore the importance of HONO for the atmospheric oxidizing capacity and the central role of cloud-aerosol interactions in aerosol formation and growth.

Supplementary material related to this article is available online at <http://www.atmos-chem-phys-discuss.net/13/23599/2013/acpd-13-23599-2013-supplement.pdf>.

Global and regional impacts of HONO on aerosol composition

Y. F. Elshorbany et al.

Title Page

Abstract

Introduction

Conclusions

References

Tables

Figures

⏪

⏩

◀

▶

Back

Close

Full Screen / Esc

Printer-friendly Version

Interactive Discussion



Acknowledgements. We would like to thank Tracey Andreae for proof reading of the manuscript. The research leading to these results has received funding from the European Research Council under the European Union's Seventh Framework Programme (FP7/2007–2013)/ERC grant agreement no. 226144.

The service charges for this open access publication have been covered by the Max Planck Society.

References

- Brühl, C., Lelieveld, J., Crutzen, P. J., and Tost, H.: The role of carbonyl sulphide as a source of stratospheric sulphate aerosol and its impact on climate, *Atmos. Chem. Phys.*, 12, 1239–1253, doi:10.5194/acp-12-1239-2012, 2012.
- Charlson, R. J., Langner, J., Rodhe, H., Leovy, C. B., and Warren, S. G.: Perturbation of the Northern Hemisphere radiative balance by backscattering from anthropogenic sulfate aerosols, *Tellus*, 43AB, 152–163, 1991.
- Charlson, R. J., Schwartz, S. E., Hales, J. M., Cess, R. D., Coakley, J. A., Hansen, J. E., and Hoffman, D. J.: Climate forcing by anthropogenic aerosols, *Science*, 255, 422–430, 1992.
- de Meij, A., Pozzer, A., Pringle, K. J., Tost, H., and Lelieveld, J.: EMAC model evaluation and analysis of atmospheric aerosol properties and distribution, with a focus on the Mediterranean region, *Atmos. Res.*, 114–115, 38–69, doi:10.1016/j.atmosres.2012.05.014, 2012.
- Dennis, R. L., Mchenry, J. N., and Barchet, W. R.: Correcting RADM's sulfate underprediction: Discovery and correction of model errors and testing the corrections through comparisons against field data, *Atmos. Environ.*, 27A, 975–997, doi:10.1016/0960-1686(93)90012-N, 1993.
- Edgerton, E., Lavery, T., Hodges, M., and Bowser, J.: National dry deposition network: Second annual progress report, Tech. rep., Environmental Protection Agency, 13127, 1990.
- Elshorbany, Y. F., Kurtenbach, R., Wiesen, P., Lissi, E., Rubio, M., Villena, G., Gramsch, E., Rickard, A. R., Pilling, M. J., and Kleffmann, J.: Oxidation capacity of the city air of Santiago, Chile, *Atmos. Chem. Phys.*, 9, 2257–2273, doi:10.5194/acp-9-2257-2009, 2009a.
- Elshorbany, Y. F., Kleffmann, J., Kurtenbach, R., Rubio, M., Lissi, E., Villena, G., Gramsch, E., Rickard, A. R., Pilling, M. J., and Wiesen, P.: Summertime photochemical ozone formation

Global and regional impacts of HONO on aerosol composition

Y. F. Elshorbany et al.

Title Page

Abstract

Introduction

Conclusions

References

Tables

Figures

◀

▶

◀

▶

Back

Close

Full Screen / Esc

Printer-friendly Version

Interactive Discussion

in Santiago, Chile, Atmos. Environ., 43, 6398–6407 doi:10.1016/j.atmosenv.2009.08.047, 2009b.

5 Elshorbany, Y. F., Kleffmann, J., Kurtenbach, R., Lissi, E., Rubio, M., Villena, G., Gramsch, E., Rickard, A. R., Pilling, M. J., and Wiesen, P.: Seasonal dependence of the oxidation capacity of the city of Santiago de Chile, Atmos. Environ., 44, 5383–5394, doi:10.1016/j.atmosenv.2009.08.036, 2010a.

Elshorbany, Y. F., Barnes, I., Becker, K. H., Kleffmann, J., and Wiesen, P.: Sources and cycling of tropospheric hydroxyl radicals – an overview, Z. Phys. Chem., 224, 967–987, doi:10.1524/zpch.2010.6136, 2010b.

10 Elshorbany, Y. F., Kleffmann, J., Hofzumahaus, A., Kurtenbach, R., Wiesen, P., Dorn, H.-P., Schlosser, E., Brauers, T., Fuchs, H., Rohrer, F., Wahner, A., Kanaya, Y., Yoshino, A., Nishida, S., Kajii, Y., Martinez, M., Rudolf, M., Harder, H., Lelieveld, J., Elste, T., Plass-Dülmer, C., Stange, G., and Berresheim, H.: HO_x Budgets during HO_xComp: a Case Study of HO_x Chemistry under NO_x limited Conditions, J. Geophys. Res., 117, D03307, doi:10.1029/2011JD017008, 2012a.

15 Elshorbany, Y. F., Steil, B., Brühl, C., and Lelieveld, J.: Impact of HONO on global atmospheric chemistry calculated with an empirical parameterization in the EMAC model, Atmos. Chem. Phys., 12, 9977–10000, doi:10.5194/acp-12-9977-2012, 2012b.

20 Feichter, J., Kjellstrom, E., Rodhe, H., Dentener, F., Lelieveld, J., and Roelofs, G.-J.: Simulation of the tropospheric sulfur cycle in a global climate model, Atmos. Environ., 30, 1693–1707, 1996.

Fortuin, J. P. F. and Kelder, H.: An ozone climatology based on ozone sonde and satellite measurements, J. Geophys. Res., 103, 31709–31734, 1998.

25 Fountoukis, C. and Nenes, A.: ISORROPIA II: a computationally efficient thermodynamic equilibrium model for K⁺, Ca²⁺, Mg²⁺, NH₄⁺, Na⁺, SO₄²⁻, NO₃⁻, Cl⁻, H₂O aerosols, Atmos. Chem. Phys., 7, 4639–4659, doi:10.5194/acp-7-4639-2007, 2007.

Ganzeveld, L., Lelieveld, J., and Roelofs, G.-J.: A dry deposition parameterization for sulfur oxides in a chemistry and general circulation model, J. Geophys. Res., 103, 5679–5694, 1998.

30 Gonçalves, M., Dabdub, D., Chang, W. L., Jorba, O., and Baldasano, J. M.: Impact of HONO sources on the performance of mesoscale air quality models, Atmos. Environ., 54, 168–176, 2012.

Global and regional impacts of HONO on aerosol composition

Y. F. Elshorbany et al.

Title Page

Abstract

Introduction

Conclusions

References

Tables

Figures

◀

▶

◀

▶

Back

Close

Full Screen / Esc

Printer-friendly Version

Interactive Discussion



- Harris, E., Sinha, B., van Pinxteren, D., Tilgner, A., Fomba, K. W., Schneider, J., Roth, A., Gnauk, T., Fahlbusch, B., Mertes, S., Lee, T., Collett, J., Foley, S., Borrmann, S., Hoppe, P., and Herrmann, H.: Enhanced role of transition metal ion catalysis during in-cloud oxidation of SO₂, *Science*, 340, 727–730, doi:10.1126/science.1230911, 2013.
- 5 Harris, G. W., Carter, W. P. L., Winer, A. M., Pitts, J. N., Platt, U., and Perner, D.: Observations of nitrous acid in the Los Angeles atmosphere and implications for predictions of ozone-precursor relationships, *Environ. Sci. Technol.*, 16, 414–419, 1982.
- Haywood, J. and O. Boucher, Estimates of the direct and indirect radiative forcing due to tropospheric aerosols: A review, *Rev. Geophys.*, 38, 513–543, doi:10.1029/1999RG000078, 10 2000.
- Hegg, D. A.: The importance of liquid-phase oxidation of SO₂ in the atmosphere, *J. Geophys. Res.*, 90, 3773–3779, 1985.
- Hjellbrekke, A.-G. and Fjæraa, A. M.: Acidifying and eutrophying compounds and particulate matter, Tech. rep., Norwegian Meteorological Institute, 13127, 2011.
- 15 Intergovernmental Panel on Climate Change, *Climate Change 2007: The Physical Science Basis*, Cambridge Univ. Press, Cambridge, UK, 2007.
- Jeuken, A.: Evaluation of chemistry and climate models using measurements and data assimilation, PhD thesis, Eindhoven University of Technology, <http://www.narcis.nl/publication/RecordID/oai:library.tue.nl:534235>, <http://alexandria.tue.nl/extra2/200001283.pdf>, 2000.
- 20 Jimenez, J. L., Canagaratna, M. R., Donahue, N. M., Prevot, A. S. H., Zhang, Q., Kroll, J. H., DeCarlo, P. F., Allan, J. D., Coe, H., Ng, N. L., Aiken, A. C., Docherty, K. S., Ulbrich, I. M., Grieshop, A. P., Robinson, A. L., Duplissy, J., Smith, J. D., Wilson, K. R., Lanz, V. A., Hueglin, C., Sun, Y. L., Tian, J., Laaksonen, A., Raatikainen, T., Rautiainen, J., Vaattovaara, P., Ehn, M., Kulmala, M., Tomlinson, J. M., Collins, D. R., Cubison, M. J., E, Dunlea, J., Huffman, J. A., Onasch, T. B., Alfarra, M. R., Williams, P. I., Bower, K., Kondo, Y., Schneider, J., Drewnick, F., Borrmann, S., Weimer, S., Demerjian, K., Salcedo, D., Cottrell, L., Griffin, R., Takami, A., Miyoshi, T., Hatakeyama, S., Shimojo, A., Sun, J. Y., Zhang, Y. M., Dzepina, K., Kimmel, J. R., Sueper, D., Jayne, J. T., Herndon, S. C., Trimborn, A. M., Williams, L. R., Wood, E. C., Middlebrook, A. M., Kolb, C. E., Baltensperger, U., and Worsnop, D. R.: Evolution of organic aerosols in the atmosphere, *Science*, 326, 1525–1529, doi:10.1126/science.1180353, 2009.
- 25 Jöckel, P., Sander, R., Kerkweg, A., Tost, H., and Lelieveld, J.: Technical Note: The Modular Earth Submodel System (MESSy) – a new approach towards Earth System Modeling, *Atmos. Chem. Phys.*, 5, 433–444, doi:10.5194/acp-5-433-2005, 2005.

Global and regional impacts of HONO on aerosol composition

Y. F. Elshorbany et al.

Title Page

Abstract

Introduction

Conclusions

References

Tables

Figures

◀

▶

◀

▶

Back

Close

Full Screen / Esc

Printer-friendly Version

Interactive Discussion

- Jöckel, P., Tost, H., Pozzer, A., Brühl, C., Buchholz, J., Ganzeveld, L., Hoor, P., Kerkweg, A., Lawrence, M. G., Sander, R., Steil, B., Stillier, G., Tanarhte, M., Taraborrelli, D., van Aardenne, J., and Lelieveld, J.: The atmospheric chemistry general circulation model ECHAM5/MESSy1: consistent simulation of ozone from the surface to the mesosphere, *Atmos. Chem. Phys.*, 6, 5067–5104, doi:10.5194/acp-6-5067-2006, 2006.
- Jöckel, P., Kerkweg, A., Pozzer, A., Sander, R., Tost, H., Riede, H., Baumgaertner, A., Grovov, S., and Kern, B.: Development cycle 2 of the Modular Earth Submodel System (MESSy2), *Geosci. Model Dev.*, 3, 717–752, doi:10.5194/gmd-3-717-2010, 2010.
- Kerkweg, A., Buchholz, J., Ganzeveld, L., Pozzer, A., Tost, H., and Jöckel, P.: Technical Note: An implementation of the dry removal processes DRY DEPosition and SEDimentation in the Modular Earth Submodel System (MESSy), *Atmos. Chem. Phys.*, 6, 4617–4632, doi:10.5194/acp-6-4617-2006, 2006.
- Kirkby, J., Curtius, J., Almeida, J., Dunne, E., Duplissy, J., Ehrhart, S., Franchin, A., Gagné, S., Ickes, L., Kürten, A., Kupc, A., Metzger, A., Riccobono, F., Rondo, L., Schobesberger, S., Tsagkogeorgas, G., Wimmer, D., Amorim, A., Bianchi, F., Breitenlechner, M., David, A., Dommen, J., Downard, A., Ehn, M., Flagan, R., Haider, S., Hansel, A., Hauser, D., Jud, W., Junninen, H., Kreissl, F., Kvashin, A., Laaksonen, A., Lehtipalo, K., Lima, J., Lovejoy, E., Makhmutov, V., Mathot, S., Mikkilä, J., Minginette, P., Mogo, S., Nieminen, T., Onnela, A., Pereira, P., Petäjä, T., Schnitzhofer, R., Seinfeld, J., Sipilä, M., Stozhkov, Y., Stratmann, F., Tomé, A., Vanhanen, J., Viisanen, Y., Aron Vrtala, A., Wagner, P., Walther, H., Weingartner, E., Wex, H., Winkler, P., Carslaw, K., Worsnop, D., Baltensperger, U., and Kulmala, M.: Role of sulphuric acid, ammonia and galactic cosmic rays in atmospheric aerosol nucleation, *Nature*, 476, 429–433, doi:10.1038/nature10343, 2011.
- Kulmala, M.: How Particles Nucleate and Grow, *Science*, 302, 1000–1001, 2003.
- Kulmala, M., Pirjola, L., and Mäkelä, J. M.: Stable sulphate clusters as a source of new atmospheric particles, *Nature*, 404, 66–69, 2000.
- Kulmala, M., Vehkamäki, H., Petäjä, T., Dal Maso, M., Lauria, A., Kerminen, V.-M., Birmili, W., and McMurry, P. H.: Formation and growth rates of ultrafine atmospheric particles: a review of observations, *J. Aerosol Sci.*, 35, 143–176, 2004.
- Kulmala, M., Lehtinen, K. E. J., and Laaksonen, A.: Cluster activation theory as an explanation of the linear dependence between formation rate of 3nm particles and sulphuric acid concentration, *Atmos. Chem. Phys.*, 6, 787–793, doi:10.5194/acp-6-787-2006, 2006.

Global and regional impacts of HONO on aerosol composition

Y. F. Elshorbany et al.

Title Page

Abstract

Introduction

Conclusions

References

Tables

Figures

◀

▶

◀

▶

Back

Close

Full Screen / Esc

Printer-friendly Version

Interactive Discussion



Lamsal, L. N., Martin, R. V., van Donkelaar, A., Celarier, E. A., Bucsele, E. J., Boersma, K. F., Dirksen, R., Luo, C., and Wang, Y.: Indirect validation of tropospheric nitrogen dioxide retrieved from the OMI satellite instrument: Insight into the seasonal variation of nitrogen oxides at northern mid latitudes, *J. Geophys. Res.*, 115, D05302, doi:10.1029/2009jd013351, 2010.

Lelieveld, J., Roelofs, G.-J., Ganzweld, L., Feichter, J., and Rodhe, H.: Terrestrial sources and distribution of atmospheric sulphur, *Phil. Trans. R. Soc. Lond. B*, 352, 149–158, 1997.

Lelieveld, J., Brühl, C., Jöckel, P., Steil, B., Crutzen, P. J., Fischer, H., Giorgetta, M. A., Hoor, P., Lawrence, M. G., Sausen, R., and Tost, H.: Stratospheric dryness: model simulations and satellite observations, *Atmos. Chem. Phys.*, 7, 1313–1332, doi:10.5194/acp-7-1313-2007, 2007.

Lelieveld, J., Barlas, C., Giannadaki, D., and Pozzer, A.: Model calculated global, regional and megacity premature mortality due to air pollution, *Atmos. Chem. Phys.*, 13, 7023–7037, doi:10.5194/acp-13-7023-2013, 2013.

Li, G., Lei, W., Zavala, M., Volkamer, R., Dusanter, S., Stevens, P., and Molina, L. T.: Impacts of HONO sources on the photochemistry in Mexico City during the MCMA-2006/MILAGO Campaign, *Atmos. Chem. Phys.*, 10, 6551–6567, doi:10.5194/acp-10-6551-2010, 2010.

Liao, H., Adams, P. J., Chung, S. H., Seinfeld, J. H., Mickley, L. G., and Jacob, D. J.: Interactions between tropospheric chemistry and aerosols in a unified general circulation model, *J. Geophys. Res.*, 108, 4001, doi:10.1029/2001JD001260, 2003.

McHenry, J. N. and Dennis, R. L.: The Relative importance of oxidation pathways and clouds to atmospheric ambient sulfate production as predicted by the regional acid deposition model, *J. Appl. Meteor.*, 33, 890–905, 1994.

Ménégoz, M., Salas y Melia, D., Legrand, M., Teyssèdre, H., Michou, M., Peuch, V.-H., Martet, M., Josse, B., and Dombrowski-Etchevers, I.: Equilibrium of sinks and sources of sulphate over Europe: comparison between a six-year simulation and EMEP observations, *Atmos. Chem. Phys.*, 9, 4505–4519, doi:10.5194/acp-9-4505-2009, 2009.

Neitola, K., Brus, D., Makkonen, U., Sipilä, M., Mauldin III, R. L., Kyllönen, K., Lihavainen, H., and Kulmala, M.: Total sulphate vs. sulphuric acid monomer in nucleation studies: which represents the “true” concentration?, *Atmos. Chem. Phys. Discuss.*, 13, 2313–2350, doi:10.5194/acpd-13-2313-2013, 2013.

Ojha, N., Naja, M., Singh, K. P., Sarangi, T., Kumar, R., Lal, S., Lawrence, M. G., Butler, T. M., and Chandola, H. C.: Variabilities in ozone at a semi-urban site in the Indo-Gangetic

Global and regional impacts of HONO on aerosol composition

Y. F. Elshorbany et al.

[Title Page](#)[Abstract](#)[Introduction](#)[Conclusions](#)[References](#)[Tables](#)[Figures](#)[◀](#)[▶](#)[◀](#)[▶](#)[Back](#)[Close](#)[Full Screen / Esc](#)[Printer-friendly Version](#)[Interactive Discussion](#)

Plain region: Association with the meteorology and regional process, *J. Geophys. Res.*, 117, D20301, doi:10.1029/2012JD017716, 2012.

Perner, D. and Platt, U.: Detection of Nitrous Acid in the Atmosphere by Differential Optical Absorption, *J. Geophys. Res.*, 6, 917–920, 1979.

5 Pozzer, A., Jöckel, P., Tost, H., Sander, R., Ganzeveld, L., Kerkweg, A., and Lelieveld, J.: Simulating organic species with the global atmospheric chemistry general circulation model ECHAM5/MESSy1: a comparison of model results with observations, *Atmos. Chem. Phys.*, 7, 2527–2550, doi:10.5194/acp-7-2527-2007, 2007.

10 Pozzer, A., Pollmann, J., Taraborrelli, D., Jöckel, P., Helmig, D., Tans, P., Hueber, J., and Lelieveld, J.: Observed and simulated global distribution and budget of atmospheric C₂-C₅ alkanes, *Atmos. Chem. Phys.*, 10, 4403–4422, doi:10.5194/acp-10-4403-2010, 2010.

Pozzer, A., de Meij, A., Pringle, K. J., Tost, H., Doering, U. M., van Aardenne, J., and Lelieveld, J.: Distributions and regional budgets of aerosols and their precursors simulated with the EMAC chemistry-climate model, *Atmos. Chem. Phys.*, 12, 961–987, doi:10.5194/acp-12-961-2012, 2012.

15 Pringle, K. J., Tost, H., Metzger, S., Steil, B., Giannadaki, D., Nenes, A., Fountoukis, C., Stier, P., Vignati, E., and Lelieveld, J.: Description and evaluation of GMXe: a new aerosol submodel for global simulations (v1), *Geosci. Model Dev.*, 3, 391–412, doi:10.5194/gmd-3-391-2010, 2010.

20 Roeckner, E., Brokopf, R., Esch, M., Giorgetta, M., Hagemann, S., Kornblueh, L., Manzini, E., Schlese, U., and Schulzweida, U.: Sensitivity of simulated climate to horizontal and vertical resolution in the ECHAM5 atmosphere model, *J. Climate*, 19, 3771–3791, 2006.

Roelofs, G. J., Lelieveld, J., and Ganzeveld, L.: Simulation of global sulfate distribution and the influence on effective cloud drop radii with a coupled photochemistry sulfur cycle model, *Tellus B*, 50, 224–242, 1998.

25 Roelofs, G. J., Kasibhatla, P., Barrie, L., Bergmann, D., Bridgeman, C., Chin, M., Christensen, J., Easter, R., Feichter, J., Jeuken, A., Kjellstrom, E., Koch, D., Land, C., Lohmann, U., and Rasch, P.: Analysis of regional budgets of sulfur species modeled for the COSAM exercise, *Tellus B*, 53, 673–694, 2001.

30 Sander, R., Kerkweg, A., Jöckel, P., and Lelieveld, J.: Technical note: The new comprehensive atmospheric chemistry module MECCA, *Atmos. Chem. Phys.*, 5, 445–450, doi:10.5194/acp-5-445-2005, 2005.

Global and regional impacts of HONO on aerosol composition

Y. F. Elshorbany et al.

Title Page

Abstract

Introduction

Conclusions

References

Tables

Figures

◀

▶

◀

▶

Back

Close

Full Screen / Esc

Printer-friendly Version

Interactive Discussion

- Sander, R., Baumgaertner, A., Gromov, S., Harder, H., Jöckel, P., Kerkweg, A., Kubistin, D., Regelin, E., Riede, H., Sandu, A., Taraborrelli, D., Tost, H., and Xie, Z.-Q.: The atmospheric chemistry box model CAABA/MECCA-3.0, *Geosci. Model Dev.*, 4, 373–380, doi:10.5194/gmd-4-373-2011, 2011.
- 5 Sandu, A. and Sander, R.: Technical note: Simulating chemical systems in Fortran90 and Matlab with the Kinetic PreProcessor KPP-2.1, *Atmos. Chem. Phys.*, 6, 187–195, doi:10.5194/acp-6-187-2006, 2006.
- Schwartz, S. E.: Aqueous-phase reactions in clouds, in: *The Chemistry of Acid Rain: Sources and Atmospheric Processes*, edited by: Johnson, R. W. and Gordon, G. E., 93–108, American Chemical Society, Symposium Series, Washington DC, 1987.
- 10 Seidl, W. and Dlugi, F.: Modelling of ionic concentrations and sulfate production in cloud droplets: use of published aerosol data, *Fresen. J. Anal. Chem.*, 340, 598–604, 1991.
- Seinfeld, J. H. and Pandis, A. N.: *Atmospheric Chemistry and Physics, From Air Pollution To Climate Change*, 2nd Edn., John Wiley & Sons, Inc., Hoboken, New Jersey, 2006.
- 15 Shen, X.: Aqueous phase sulphate production in clouds at mt. Tai in eastern China, thesis, Colorado State university, US, http://digitool.library.colostate.edu/R/?func=dbin-jump-full&object_id=127482&local_base=GEN01, 2011.
- Sun, Y. L., Wang, Z. F., Fu, P. Q., Yang, T., Jiang, Q., Dong, H. B., Li, J., and Jia, J. J.: Aerosol composition, sources and processes during wintertime in Beijing, China, *Atmos. Chem. Phys.*, 13, 4577–4592, doi:10.5194/acp-13-4577-2013, 2013.
- 20 Tost, H. and Pringle, K. J.: Improvements of organic aerosol representations and their effects in large-scale atmospheric models, *Atmos. Chem. Phys.*, 12, 8687–8709, doi:10.5194/acp-12-8687-2012, 2012.
- Tost, H., Jöckel, P., Kerkweg, A., Sander, R., and Lelieveld, J.: Technical note: A new comprehensive SCAVenging submodel for global atmospheric chemistry modelling, *Atmos. Chem. Phys.*, 6, 565–574, doi:10.5194/acp-6-565-2006, 2006.
- 25 Tost, H., Jöckel, P., Kerkweg, A., Pozzer, A., Sander, R., and Lelieveld, J.: Global cloud and precipitation chemistry and wet deposition: tropospheric model simulations with ECHAM5/MESSy1, *Atmos. Chem. Phys.*, 7, 2733–2757, doi:10.5194/acp-7-2733-2007, 2007.
- 30 Totsuka, T., Sase, H., and Shimizu, H.: Major activities of acid deposition monitoring network in East Asia (EANET) and related studies, in: *Plant Responses to Air Pollution and Global*

Global and regional impacts of HONO on aerosol composition

Y. F. Elshorbany et al.

Title Page

Abstract

Introduction

Conclusions

References

Tables

Figures

◀

▶

◀

▶

Back

Close

Full Screen / Esc

Printer-friendly Version

Interactive Discussion



Change, edited by: Omasa, K., Nouchi, I., and DeKok, L. J., Springer-Verlag, Tokyo, 251–259, 13127, doi:10.1007/4-431-31014-2_28, 2005.

van Aalst, M. K., van den Broek, M. M. P., Bregman, A., Brühl, C., Steil, B., Toon, G. C., Garcelon, S., Hansford, G. M., Jones, R. L., Gardiner, T. D., Roelofs, G. J., Lelieveld, J., and Crutzen, P.J.: Trace gas transport in the 1999/2000 Arctic winter: comparison of nudged GCM runs with observations, *Atmos. Chem. Phys.*, 4, 81–93, doi:10.5194/acp-4-81-2004, 2004.

Van den Berg, A., Dentener, F. J., and Lelieveld, J.: Modelling the chemistry of the marine boundary layer: Sulfate formation and the role of sea-salt aerosol particles, *J. Geophys. Res.*, 105, 11671–11698, 2000.

Venkataraman, C., Mehra, A., and Mhaskar, P.: Mechanisms of sulphate aerosol production in clouds: effect of cloud characteristics and season in the Indian region, *Tellus*, 53B, 260–272, 2001.

Vignati, E., Wilson, J., and Stier, P.: M7: an efficient size resolved aerosol microphysics module for large-scale aerosol transport models, *J. Geophys. Res.*, 109, D22202, doi:10.1029/2003JD004485, 2004.

World Health Organization, World health report 2002, technical report, Geneva, Switzerland, 2002.

Zhang, L., Jacob, D. J., Knipping, E. M., Kumar, N., Munger, J. W., Carouge, C. C., van Donkelaar, A., Wang, Y. X., and Chen, D.: Nitrogen deposition to the United States: distribution, sources, and processes, *Atmos. Chem. Phys.*, 12, 4539–4554, doi:10.5194/acp-12-4539-2012, 2012.

Zhang, R., Sarwar, G., Fung, J. C. H., Lau, A. K. H., and Zhang, Y.: Examining the impact of nitrous acid chemistry on ozone and PM over the Pearl River Delta Region, *Adv. Meteorol.*, 2012, 140932, doi:10.1155/2012/140932, 2012.

Table 1. Contributions of the different chemical processes to the simulated aerosol sulphate, nitrate and ammonium concentrations and their relative enhancement as a result of simulating realistic HONO levels during January in the eastern US and China.

species	conditions	eastern US, 95–65° W, 30–50° N			eastern China, 100–130° E, 25–55° N		
		base_S [$\mu\text{g m}^{-3}$]	S [$\mu\text{g m}^{-3}$]	% ¹	base_S [$\mu\text{g m}^{-3}$]	S [$\mu\text{g m}^{-3}$]	% ¹
total sulphate	S1	2.97	3.39	14	5.18	5.72	11
	S2	2.23	2.92	31	2.36	3.17	34
	S3	2.47	2.38	−3.7	4.26	4.23	−0.61
	H ₂ SO ₄ % ²	17	30		18	26	
	Aqueous % ³	25	14		54	45	
chemically formed sulphate	H ₂ SO ₄ %	41	68		25	37	
	Aqueous %	59	32		75	63	
nitrate	S1	2.05	2.23	8.9	2.51	2.64	4.9
	S2	2.41	2.61	8.4	3.20	3.25	1.6
	S3	1.79	1.89	5.9	2.40	2.45	2.4
ammonium	S1	1.08	1.25	16	2.97	3.18	7.1
	S2	0.77	1.05	37	1.56	1.87	20
	S3	0.88	0.86	−1.8	2.60	2.53	−2.8
number concentration		base_S [cm^{-3}]	S [cm^{-3}]	% ¹	base_S [cm^{-3}]	S [cm^{-3}]	% ¹
	S1	2032	2242	10	5520	6129	11
	S2	2129	2675	26	5830	9857	69
	S3	1956	1951	−0.26	5438	5430	−0.15

S1: basic setup, all aerosol formation processes are included, S2: no aqueous phase chemistry, i.e., only uptake of gaseous species based on Henry's law coefficients, S3: no gas phase production of H₂SO₄ from the oxidation of SO₂ with OH.

¹ Relative enhancement as a result of simulating realistic HONO levels.

² Relative contribution of the gas phase H₂SO₄, calculated from the difference between S1 and S3.

³ Relative contribution of the aqueous phase chemistry, calculated from the difference between S1 and S2.

Title Page

Abstract

Introduction

Conclusions

References

Tables

Figures

◀

▶

◀

▶

Back

Close

Full Screen / Esc

Printer-friendly Version

Interactive Discussion



Global and regional impacts of HONO on aerosol composition

Y. F. Elshorbany et al.

Table 2. Contributions of the different aerosol modes to the simulated aerosol mean sulphate, nitrate and ammonium concentrations and their relative enhancement as a result of simulating realistic HONO levels.

aerosol mode	date	sulphate				nitrate				ammonium			
		eastern US ¹		eastern China ²		eastern US ¹		eastern China ²		eastern US ¹		eastern China ²	
		$\mu\text{g m}^{-3}$	%*	$\mu\text{g m}^{-3}$	%*	$\mu\text{g m}^{-3}$	%*	$\mu\text{g m}^{-3}$	%*	$\mu\text{g m}^{-3}$	%*	$\mu\text{g m}^{-3}$	%*
total aerosol	January	2.97	14	5.18	11	2.05	9	2.51	5	1.07	16	2.97	7
	July	3.07	2	3.70	1	0.49	-7	0.45	-8	0.89	3	1.18	1
ns	January	6.13×10^{-7}	1021	4.74×10^{-7}	9090	8.79×10^{-13}	4564	1.56×10^{-11}	528 353	1.90×10^{-07}	1098	1.59×10^{-07}	10 303
	July	7.04×10^{-9}	-20	4.31×10^{-8}	7	2.85×10^{-18}	-85	3.88×10^{-15}	-100	1.67×10^{-09}	-24	1.51×10^{-08}	6
ks	January	1.07×10^{-2}	65	1.47×10^{-2}	29	3.94×10^{-06}	134	1.76×10^{-05}	36	3.59×10^{-03}	75	4.79×10^{-03}	35
	July	1.24×10^{-2}	1	2.03×10^{-2}	4	2.46×10^{-12}	-29	3.43×10^{-11}	18	4.42×10^{-03}	3	6.41×10^{-03}	4
as	January	1.17	31	3.27	18	1.08	23	1.58	13	0.75	25	2.13	14
	July	2.22	2	2.61	0.9	0.26	-5	0.26	-10	0.79	3	0.99	1
cs	January	1.79	2	1.89	-3	0.97	-7	0.93	-8	0.32	-6	0.84	-10
	July	0.83	1	1.07	2	0.23	-9	0.19	-5	0.09	3	0.18	1

* Relative enhancement as a result of simulating realistic HONO levels. Abbreviations *ns, ks, as and cs* refer to nucleation, Aitken, accumulation and coarse soluble aerosol modes, respectively. Data averaged over the eastern.

¹ US (95–65° W, 30–50° N) and ² China (100–130° E, 25–55° N).

Title Page

Abstract Introduction

Conclusions References

Tables Figures

⏪ ⏩

◀ ▶

Back Close

Full Screen / Esc

Printer-friendly Version

Interactive Discussion



Global and regional impacts of HONO on aerosol composition

Y. F. Elshorbany et al.

Title Page

Abstract

Introduction

Conclusions

References

Tables

Figures

◀

▶

◀

▶

Back

Close

Full Screen / Esc

Printer-friendly Version

Interactive Discussion



Table 3. Contributions of the different aerosol modes to the simulated mean aerosol number concentrations and their relative enhancement as a result of simulating realistic HONO levels during January.

aerosol mode	run	aerosol number concentration			
		eastern US ¹		eastern China ²	
		cm ⁻³	%*	cm ⁻³	%*
total aerosol	S1	2032	10	5520	11
	S3	1956	-0.3	5438	-0.1
ns	S1	8.51	681	10.4	5131
	S3	7.59×10^{-4}	48	1.07×10^{-3}	-37
ks	S1	552	44	825	31
	S3	358	2	550	1
as	S1	235	27	567	14
	S3	148	1	369	2
cs	S1	1.40	0.6	2.61	-2
	S3	1.33	0.2	2.70	-4
ki	S1	1235	-13	4075	-6
	S3	1448	-1	4472	-1
ai	S1	5.97×10^{-3}	-38	33.9	2
	S3	1.15×10^{-1}	-2	39.1	2
ci	S1	1.08×10^{-3}	-30	2.74	2
	S3	5.73×10^{-3}	-1	3.10	1

* Relative enhancement as a result of simulating realistic HONO levels (S1 run). Abbreviations "ns, ks, as and cs" refer to nucleation, Aitken, accumulation and coarse soluble aerosol modes, respectively, while "ki, ai and ci" refer to the corresponding insoluble modes. Data are averaged over the eastern ¹ US (95–65° W, 30–50° N) and ² China (100–130° E, 25–55° N).

Global and regional impacts of HONO on aerosol composition

Y. F. Elshorbany et al.

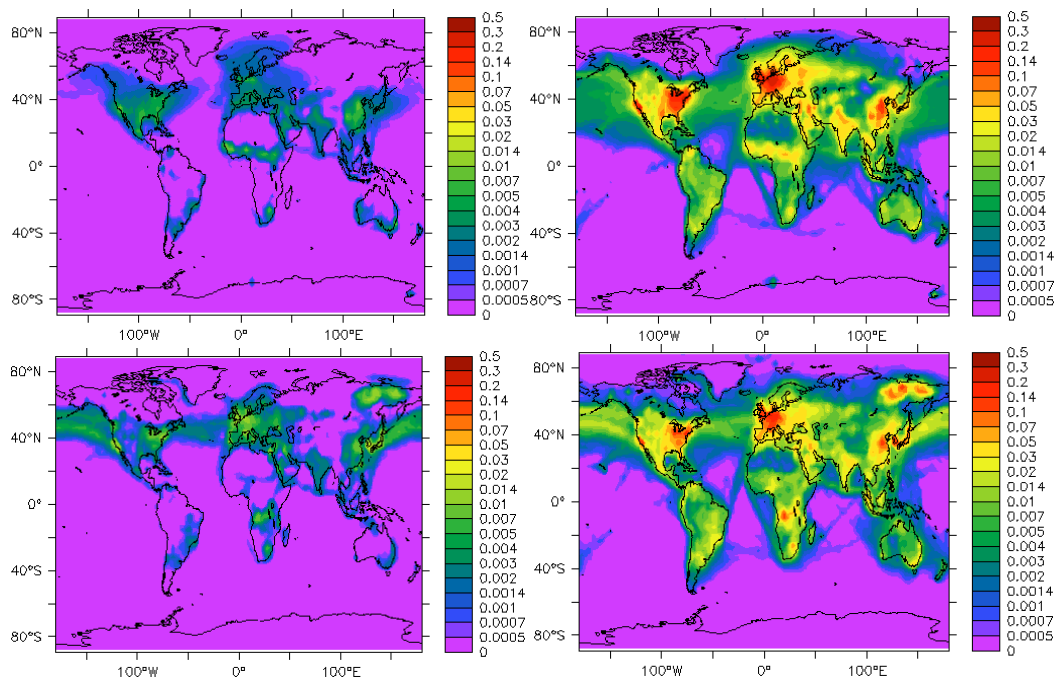


Fig. 1. Simulated monthly average HONO mixing ratios (ppbv) from the reference run (base_S1, left) and the sensitivity run (S1, i.e., using a HONO/NO_x ratio of 0.02) near the surface in January (upper panels) and July (lower panels).

[Title Page](#)[Abstract](#)[Introduction](#)[Conclusions](#)[References](#)[Tables](#)[Figures](#)[◀](#)[▶](#)[◀](#)[▶](#)[Back](#)[Close](#)[Full Screen / Esc](#)[Printer-friendly Version](#)[Interactive Discussion](#)

Global and regional impacts of HONO on aerosol composition

Y. F. Elshorbany et al.

Title Page

Abstract

Introduction

Conclusions

References

Tables

Figures



Back

Close

Full Screen / Esc

Printer-friendly Version

Interactive Discussion

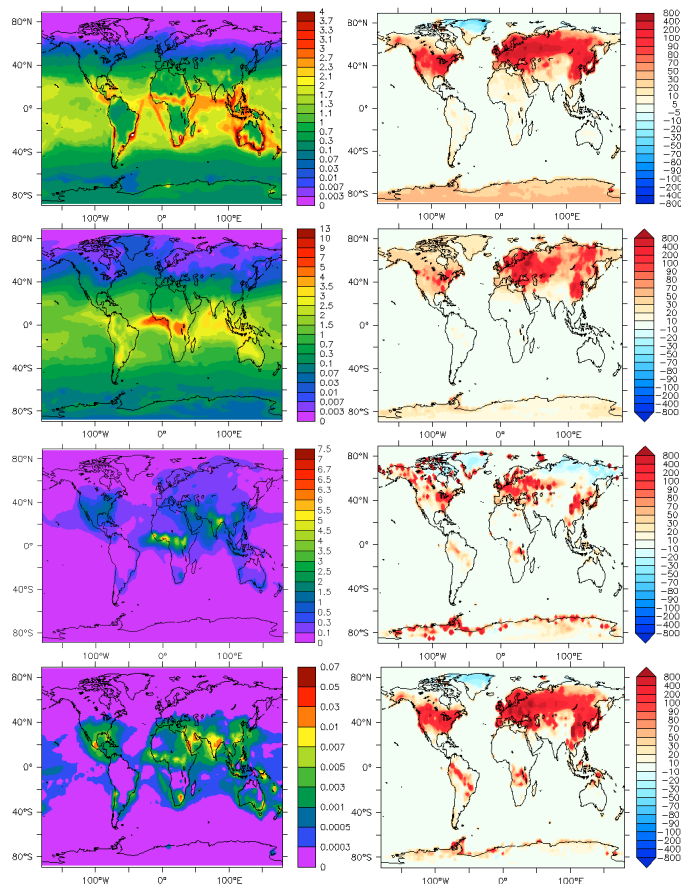


Fig. 2. Average simulated OH (from top to bottom) (10^6 molecules cm^{-3}), H_2O_2 , HNO_3 , H_2SO_4 (ppbv) near the surface from the reference run (left panels) and their relative enhancements (%) by using a HONO/ NO_x ratio of 0.02 (right panels) in January.

Global and regional impacts of HONO on aerosol composition

Y. F. Elshorbany et al.

Title Page

Abstract

Introduction

Conclusions

References

Tables

Figures

◀

▶

◀

▶

Back

Close

Full Screen / Esc

Printer-friendly Version

Interactive Discussion

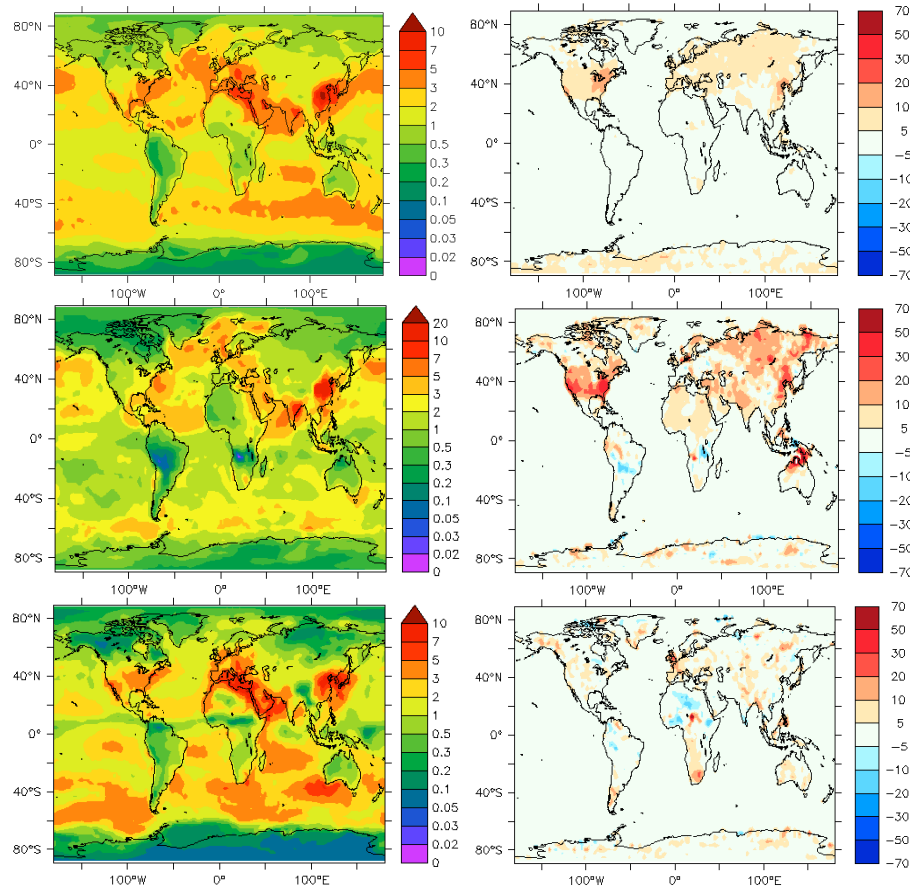


Fig. 3. Simulated aerosol sulphate concentrations ($\mu\text{g m}^{-3}$) near the surface for the mean annual (upper panels), boreal winter (January, middle panels) and summer (July, lower panels) conditions from the reference run (base_S1) and relative enhancements (in %, right panels) due to HONO enhancement in the model.

Global and regional impacts of HONO on aerosol composition

Y. F. Elshorbany et al.

Title Page

Abstract

Introduction

Conclusions

References

Tables

Figures



Back

Close

Full Screen / Esc

Printer-friendly Version

Interactive Discussion

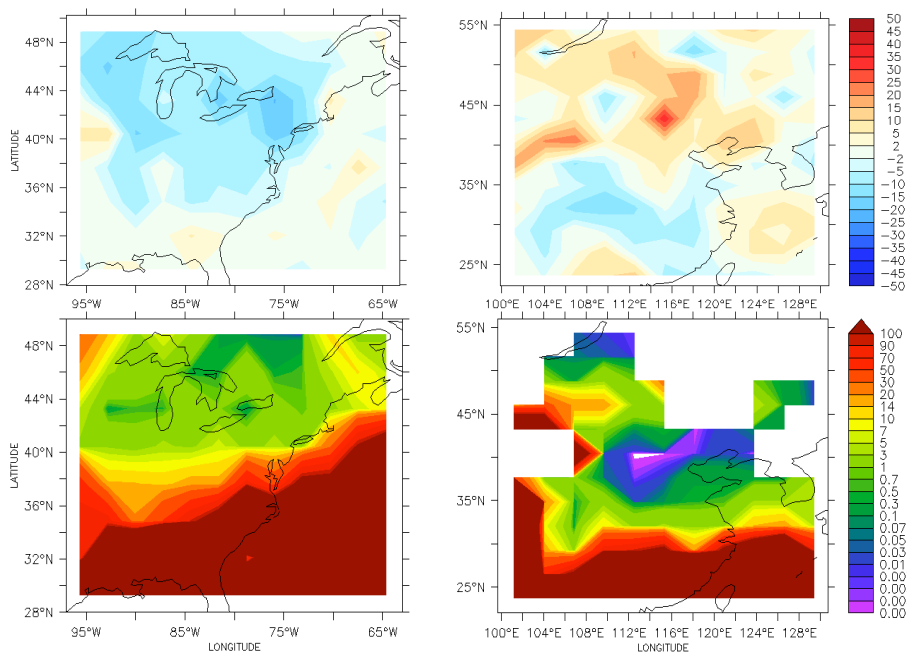


Fig. 4. Simulated monthly average relative enhancements (%) of aerosol sulphate (upper panels), and the ratio of in-cloud aqueous phase concentrations of $\text{H}_2\text{O}_2/\text{HSO}_3^-$ (lower panels) in January without the gas phase oxidation of SO_2 (base_S3), over the eastern US (left) and China (right).

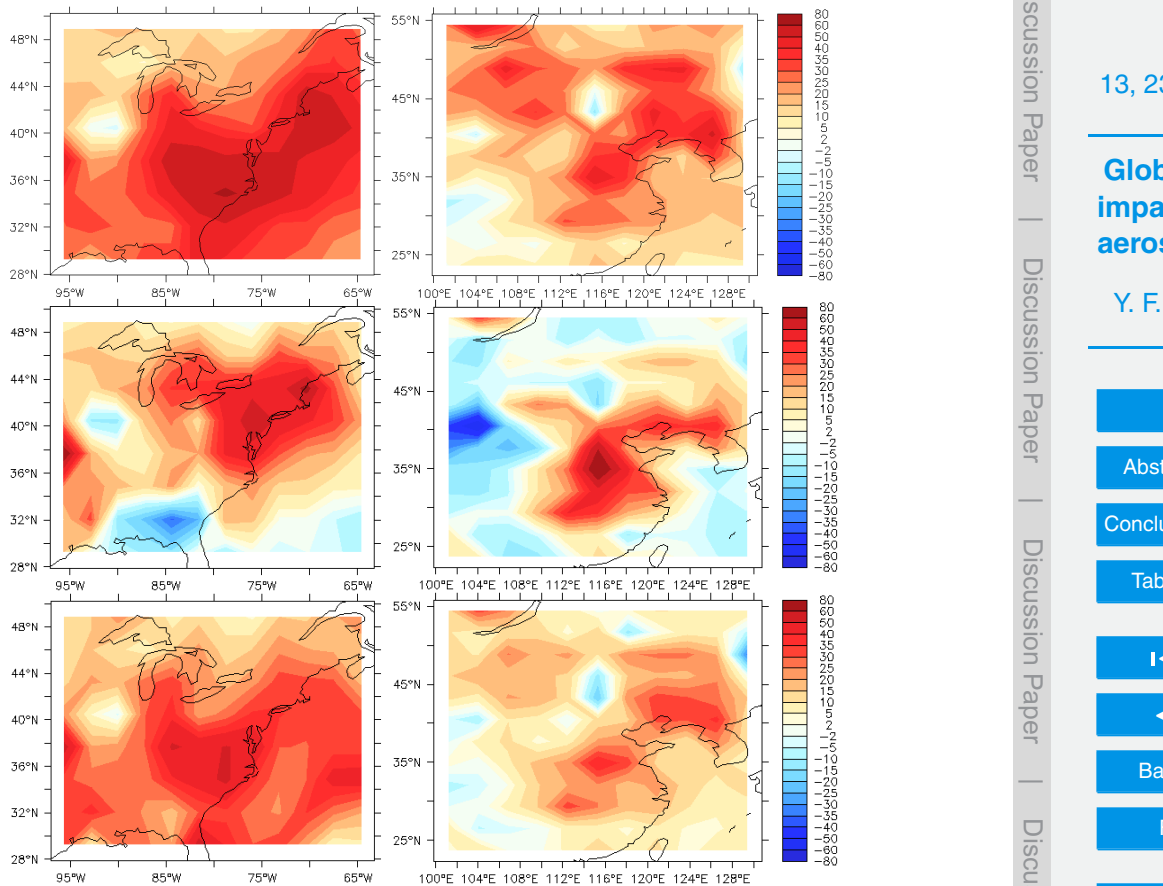


Fig. 5. Simulated monthly average relative enhancements (%) in the aerosol (accumulation soluble mode, as) sulphates (upper panels), nitrates (middle panels) and ammonium (lower panels) near the surface in January over the eastern US (left) and China (right).

Global and regional impacts of HONO on aerosol composition

Y. F. Elshorbany et al.

Title Page

Abstract Introduction

Conclusions References

Tables Figures

◀ ▶

◀ ▶

Back Close

Full Screen / Esc

Printer-friendly Version

Interactive Discussion



Global and regional impacts of HONO on aerosol composition

Y. F. Elshorbany et al.

Title Page

Abstract

Introduction

Conclusions

References

Tables

Figures



Back

Close

Full Screen / Esc

Printer-friendly Version

Interactive Discussion

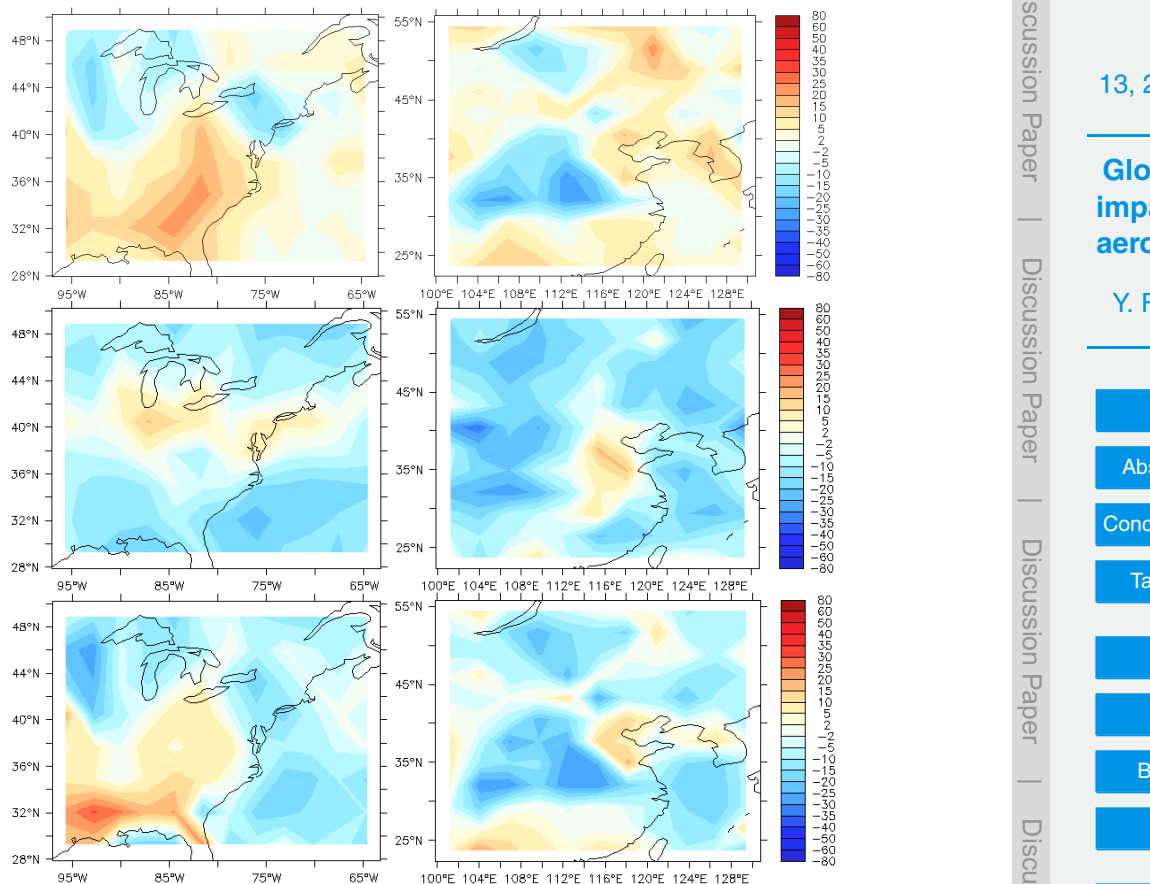


Fig. 6. Simulated monthly average relative enhancements (%) in the aerosol (coarse soluble mode, cs) sulphates (upper panels), nitrates (middle panels) and ammonium (lower panels) near the surface in January over the eastern US (left) and China (right).

Global and regional impacts of HONO on aerosol composition

Y. F. Elshorbany et al.

Title Page

Abstract

Introduction

Conclusions

References

Tables

Figures

◀

▶

◀

▶

Back

Close

Full Screen / Esc

Printer-friendly Version

Interactive Discussion

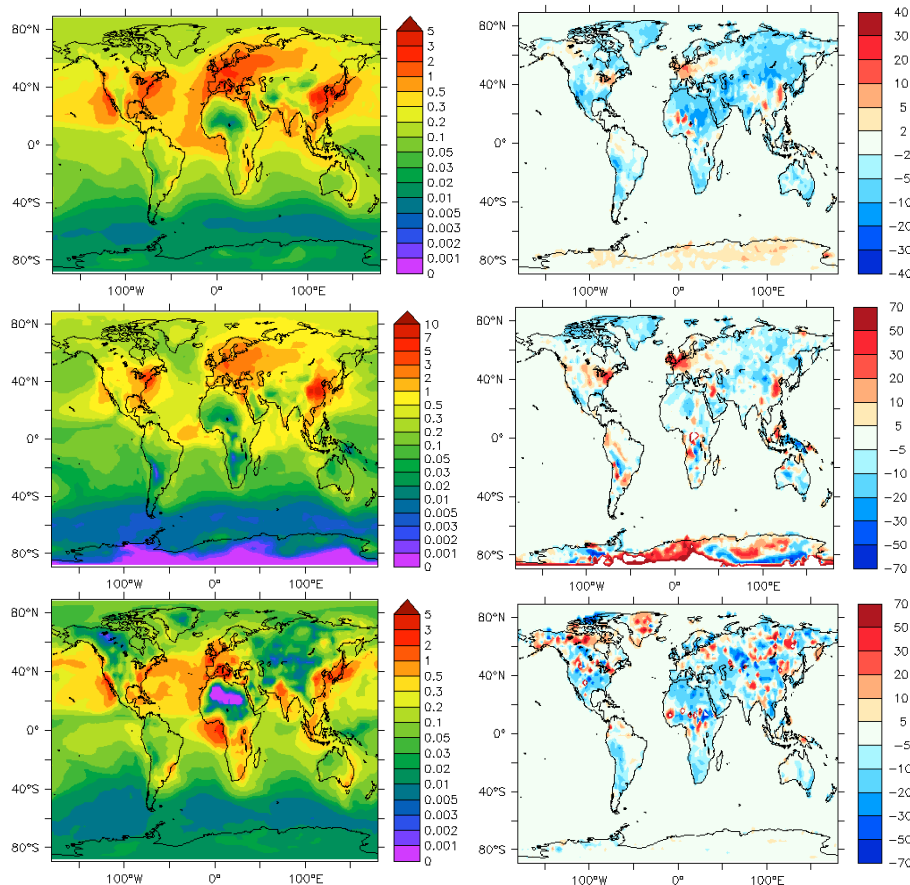


Fig. 7. Simulated aerosol nitrate concentration ($\mu\text{g m}^{-3}$) near the surface for the mean annual (upper panels), boreal winter (January, middle panels) and summer (July, lower panels) conditions and relative enhancements (in %, right panels) due to HONO enhancement in the model.

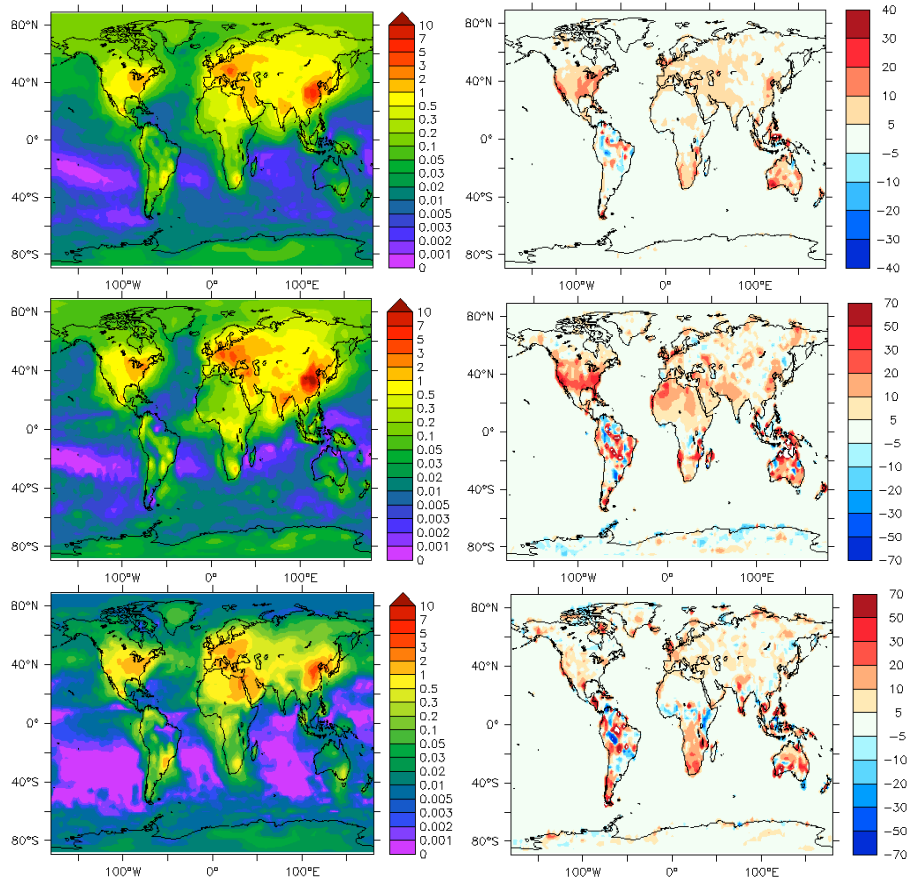


Fig. 8. Simulated aerosol ammonium concentration ($\mu\text{g m}^{-3}$) near the surface for the mean annual (upper panels), boreal winter (January, middle panels) and summer (July, lower panels) conditions and relative enhancements (in %, right panels) due to HONO enhancement in the model.

Title Page

Abstract Introduction

Conclusions References

Tables Figures

◀ ▶

◀ ▶

Back Close

Full Screen / Esc

Printer-friendly Version

Interactive Discussion



Global and regional impacts of HONO on aerosol composition

Y. F. Elshorbany et al.

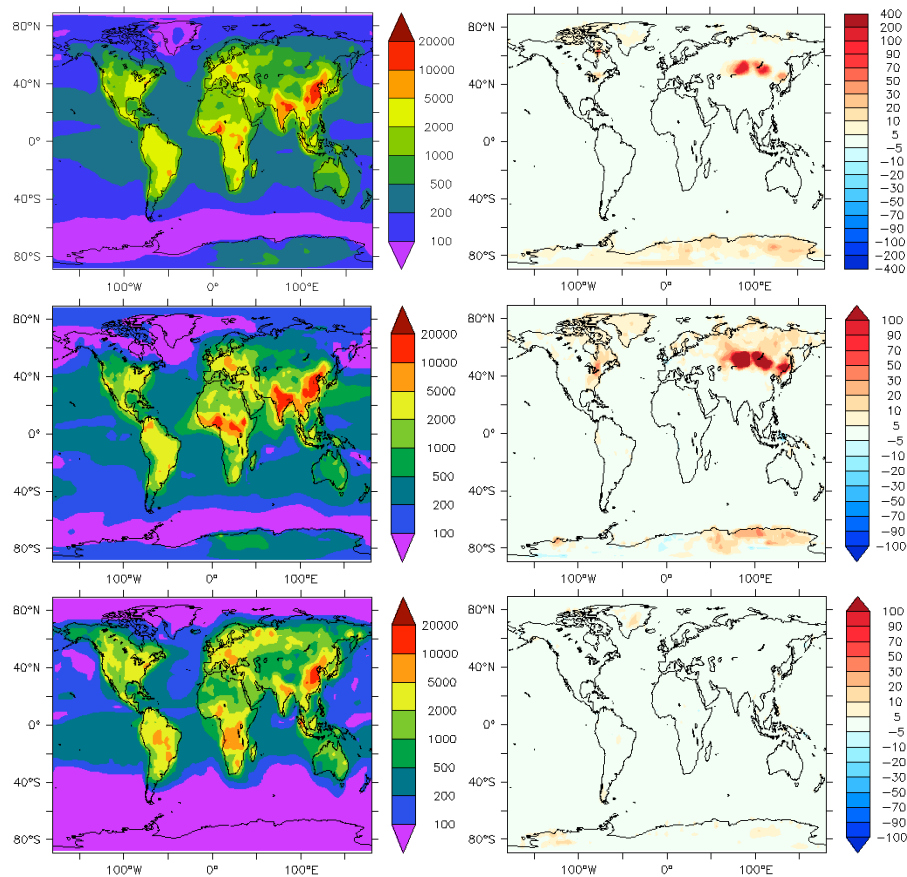


Fig. 9. Simulated mean aerosol number concentrations (cm^{-3}) near the surface for the mean annual (upper panels), boreal winter (January, middle panels) and summer (July, lower panels) conditions and relative enhancements (in %, right panels) due to HONO enhancement in the model.

Global and regional impacts of HONO on aerosol composition

Y. F. Elshorbany et al.

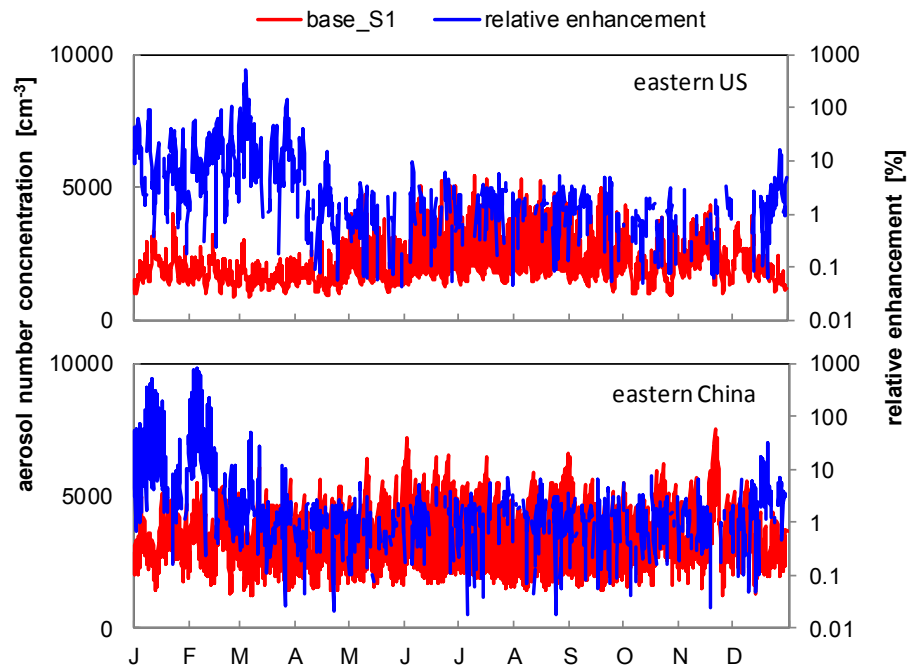


Fig. 10. Simulated aerosol number concentrations and the relative enhancement related to simulating realistic HONO levels near the surface over the eastern US (95–65° W and 30–50° N, upper panels) and China (100–130° E and 25–55° N, lower panels).

[Title Page](#)[Abstract](#)[Introduction](#)[Conclusions](#)[References](#)[Tables](#)[Figures](#)[◀](#)[▶](#)[◀](#)[▶](#)[Back](#)[Close](#)[Full Screen / Esc](#)[Printer-friendly Version](#)[Interactive Discussion](#)

Global and regional impacts of HONO on aerosol composition

Y. F. Elshorbany et al.

Title Page

Abstract

Introduction

Conclusions

References

Tables

Figures

◀

▶

◀

▶

Back

Close

Full Screen / Esc

Printer-friendly Version

Interactive Discussion

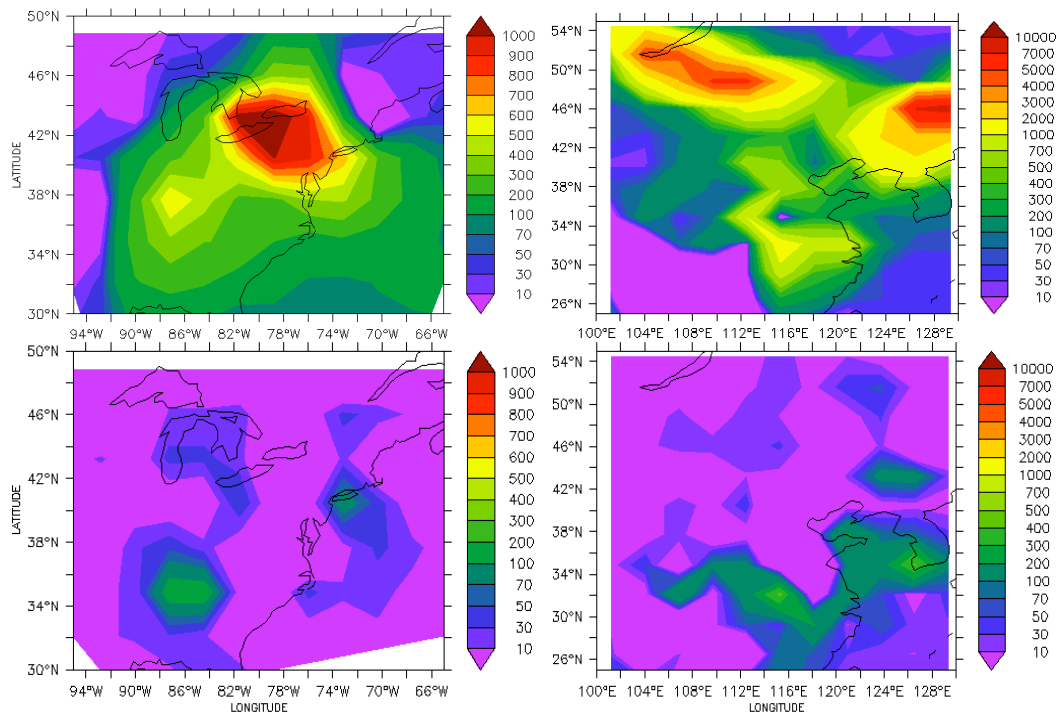


Fig. 11. Simulated monthly mean enhancement in the aerosol number concentrations (cm^{-3}) near the surface over the eastern US (left) and China (right) during winter (January, upper panels) and summer (July, lower panels) due to HONO enhancement in the model.